

FAST AMERICAN OPTION PRICING:

THE DOUBLE- BOUNDARY CASE

Leif Andersen and Mark Lake consider how to adjust integral-based numerical techniques for American options to the special situation where the exercise region has a “double boundary.” [➤](#)



OPTION PRICING

In this article, we consider how to adjust integral-based numerical techniques for American options to the special situation where the exercise region has a “double boundary.” This circumstance can arise when rates and dividend yields are negative, something that is not an unlikely event in the present market environment.

While the principles at play are generic, for concreteness we focus on the specific algorithm in [1] which was described in detail by Mike Staunton in a recent article in *Wilmott* (see [14]). Working primarily in a Black–Scholes setting, we develop new results and completely characterize the topology of the optimal exercise region; establish short- and long-term asymptotics for all possible configurations of the signs of rates and dividend yields; and provide a complete numerical algorithm for the pricing of American puts and calls with a double exercise boundary. The algorithm is carefully formulated such that each of the two exercise boundaries can be computed separately from each other, which not only simplifies implementation but also allows us to retain the high accuracy of the work in [1].

Introduction

In Andersen *et al.* [1], we introduced a fast, and very accurate, numerical technique for American option prices. Loosely, the method involves fixed-point iterations for the early-exercise boundary of the option, aided by a Chebyshev collocation scheme and high-performance quadrature routines. As shown in [1], the resulting algorithm achieves spectral convergence rates and allows for high-accuracy pricing of hundreds of thousands¹ of American option prices per second. An implementation in Visual Basic of the algorithm was written by Mike Staunton and published in *Wilmott* in July 2020, see [14].

As written in [1], the American option pricing algorithm hinges on certain parameter assumptions to function properly. Most importantly, the algorithm relies on the boundary between the exercise and continuation regions of the American

All in all, one concludes that it has become important that American option pricing algorithms be able to handle arbitrary combinations of signs of rates and dividends

option being a single smooth function of maturity, well represented by a Chebyshev polynomial.² This can, however, be violated for various reasons. For instance, if the underlying asset pays discrete dividends, the exercise boundary of the American put option will typically only be *piecewise* smooth. This situation can be handled by, essentially, splitting the scheme of [1] into segments, running backwards from one dividend date to the previous one.³ Another difficulty – and the one we will focus on in this article – can arise if interest rates and dividend yields are negative, a situ-

ation that was explicitly excluded from [1]. In this case, the boundary that separates exercise from continuation can sometimes cease to be a single function of time, requiring instead (if the boundary exists at all) *two* functions of time, giving rise to a “double-boundary” or, synonymously, a “double-continuation region” (see [2]).

Though assumed away in [1], negative interest rates have, in fact, become a common occurrence in recent times. In addition, it is often also the case that dividend yields will, effectively, be negative. For instance, for American FX options the “dividend yield” in the pricing model is, of course, the foreign currency interest rate – which can be negative for the same reasons the discounting (domestic) interest rate can. Even for equity options, incorporation of basis or funding spreads into the dynamic asset models can also easily result in situations where stock forwards are above levels implied by the chosen risk-free discounting rate, in effect producing a negative dividend yield. In [2], several examples of (effectively) negative rates and dividend yields are also discussed in the context of real options.

All in all, one concludes that it has become important that American option pricing algorithms be able to handle arbitrary combinations of signs of rates and dividends. In this article, we demonstrate how to do this for the algorithm in [1], providing in particular a complete recipe for the necessary updates of any computer implementation (such as that of [14]) to handle the double-boundary case.

It is our aim to be succinct and keep the article short, but we need a few prerequisites and results to ensure that the reader can make sense of the necessary algorithmic changes. For this, we first establish some fundamental results for American option exercise boundaries, with a special focus on the cases where a double boundary might arise. For both puts and calls, we establish once and for all the topology of the exercise region, along with short- and long-maturity asymptotics, for all possible sign combinations of rates and dividends. Then we extend the integral representations for the American option value to arbitrary exercise regions, a result that is then used for the adaptation of the algorithm in [1] to the double-boundary case, as well as to certain edge cases that require additional care. Numerical results are presented next, followed by the concluding discussion of possible extensions of our results. Appendix A lists some useful results for perpetual American options with negative rates and dividends.

The American option exercise region

For simplicity, our setting is Black–Scholes with constant parameters. That is, the risk-neutral asset price process is

$$\frac{dS(t)}{S(t)} = (r - q) dt + \sigma dW(t),$$

where $W(t)$ is a standard Wiener process, and the risk-free rate r , continuous dividend yield q , and volatility $\sigma > 0$ are all assumed constant. Since the process is *time-homogeneous*, the price at time t of an option with maturity T is a function of $\tau \triangleq T - t$ and $S = S(t)$, independent of t . We denote the price of an American option by $V(\tau, S)$; the corresponding European price is denoted $v(\tau, S)$. For put and call options with strike $K > 0$, of course:

$$v(\tau, S) = \eta S e^{-q\tau} \Phi(\eta d_+) - \eta K e^{-r\tau} \Phi(\eta d_-),$$

where η is +1 for a call and –1 for a put, and

OPTION PRICING

$$d_{\pm} = \frac{\ln(S/K) + (r - q \pm \frac{\sigma^2}{2})\tau}{\sigma\sqrt{\tau}}, \quad \Phi(x) = \frac{1}{\sqrt{2\pi}} \int_{-\infty}^x e^{-y^2/2} dy.$$

Call and put prices are known to be convex functions⁴ of S and of K ; and if volatility is strictly positive, the convexity is strict for American options when the option is alive (i.e., prior to maturity and outside the early-exercise region). It follows trivially that the set (i.e., the *exercise region*) of $S(t)$ at which an American call option price is equal to the exercise value $S(t) - K$ (a linear function of $S(t)$) must be an interval on (K, ∞) , which can either be: (i) *empty* (no early exercise); (ii) *half-infinite* (one exercise boundary); or (iii) *finite* (two exercise boundaries).

The third case mentioned above (the double boundary) is likely unfamiliar to many, so let us proceed to provide some intuition for the circumstances under which two exercise boundaries might arise.

Short-maturity analysis

For any American option, the value function will be an increasing function of maturity T , an obvious consequence of the fact that increasing the maturity of the option will expand the set of possible exercise times for the option. For the time-homogenous Black–Scholes model, this translates into $\partial V(\tau, S) / \partial \tau \geq 0$ where it is not hard to show that the inequality is strict if S is in the *continuation region* (i.e., the region in S -space where it is *not* optimal to exercise). As such, extending the maturity τ of the option in our Black–Scholes model will never cause the option value to move from outside the exercise region (where the option is larger than the intrinsic value) to inside the exercise region (where the option is equal to intrinsic value), although the opposite is always possible. In other words, the exercise interval discussed above will (if it exists in the first place) contract as τ is increased.⁵

It follows from the discussion above that one expects the exercise interval to be at its widest – and most striking, so to speak – for small values of τ , hence we first consider a small- τ analysis. Focusing initially on an American call option, we set $\tau = \delta$, with δ being an infinitesimally small quantity (our treatment here is informal). Skipping argument t , let $S = S(t)$ and assume $S > K$ (with $K > 0$), such that a decision to exercise early will yield a non-zero amount $S - K$. On the contrary, if we decide *not* to exercise early, we get, after factoring in discounting and dividend payments, $S(1 - q\delta) - K(1 - r\delta) = S - K + \delta(rK - qS)$. Comparing the proceeds from exercise and non-exercise, we see that exercise is only optimal if the following two inequalities are *simultaneously* satisfied:

$$rK - qS < 0, \quad S > K. \quad (1)$$

To see the implications of (1), consider three possible cases⁶ for q :

- $q > 0$: For positive q we can rearrange (1) to see that exercise just prior to maturity is optimal if $S > K \max(1, r/q)$ (i.e., we always have a single exercise boundary).
- $q = 0$: Clearly, if $q = 0$ and $r \geq 0$, (1) is never satisfied (i.e., no exercise boundary); but if $q = 0$ and $r < 0$ we exercise if $S > K$ (i.e., a single exercise boundary).
- $q < 0$: If $q < 0$ and $r \geq 0$, (1) is never satisfied (i.e., no exercise boundary). However, if $q < 0$ and $r < 0$, then the exercise condition is $S \in (K, Kr/q)$. This

set is empty if $0 > r \geq q$, but if $r < q < 0$, we get a lower exercise bound of K and an upper bound of Kr/q (i.e., we now have a *double* exercise boundary).

The analysis above was for the American call option. For the American put, the exercise condition just prior to maturity is easily shown to be

$$qS - rK < 0, \quad S < K, \quad (2)$$

where of course we also know that $S > 0$ in the Black–Scholes model. For the American put, the double-boundary case arises when $q < r < 0$ with the exercise region being the interval $S \in (Kr/q, K)$. Notice that (2) emerges from (1) by interchanging S with K , and r with q , a general (and very convenient) result known as *put–call symmetry* [see (18) and (19) for a more precise statement of the result].

Long-maturity analysis

As we explained above, as τ is increased in our model, the exercise region, if it exists, will contract. If the exercise region does not exist for some τ , it is also easily verified (by the same arguments as we used above) that it cannot spring into existence solely by increasing τ . So, for those cases where exercise is never optimal just prior to maturity, it follows that exercise is never optimal for *any* maturity. In contrast, for cases where an exercise region exists just prior to maturity, it is conceivable that there are finite times when the exercise regions may ultimately disappear altogether. For instance, for the double-boundary case one could imagine that there can sometimes be a finite maturity τ^* where the two exercise boundaries, B and Y , say, become identical, $B(\tau^*) = Y(\tau^*)$ effectively “pinching off” the exercise region completely for all $\tau > \tau^*$.

To establish whether exercise regions can disappear in the manner described above, and, more generally, to find useful asymptotic levels for the exercise region for large τ , it is convenient to study *perpetual* American options. An analysis of the cases relevant to this article is available in Appendix A, which, when combined with the short-time asymptotics described in the subsection above, allows us to show a variety of results about the exercise boundaries at finite times.

To illustrate, consider for now only the double-boundary case, and, for both puts and calls, let us denote the boundary nearer to the strike K by $B(\tau^*)$ and the more distant one by $Y(\tau)$. For puts and calls, we showed that when there are two boundaries, then

$$B_0 = B(0+) = K, \quad Y_0 = Y(0+) = Kr/q.$$

When the limits exist, let us also denote

$$B_{\infty} = \lim_{\tau \rightarrow \infty} B(\tau), \quad Y_{\infty} = \lim_{\tau \rightarrow \infty} Y(\tau).$$

We can now definitively answer the question of whether the boundaries intersect:

Proposition 1. *Let $\sigma^* = |\sqrt{-2r} - \sqrt{-2q}|$. For the American double-boundary case (i.e., $r < q < 0$ for calls and $q < r < 0$ for puts), the following are true:*

1. *If $\sigma > \sigma^*$, B_{∞} and Y_{∞} do not exist, and the boundaries B and Y therefore intersect at a finite τ^* .*



OPTION PRICING

- If $\sigma < \sigma^*$, the boundaries do not intersect for any τ . B_∞ and Y_∞ exist; have closed-form expressions (see Tables 1 and 2); and satisfy
call: $K < B_\infty < K\sqrt{r/q} < Y_\infty < Kr/q$,
put: $K > B_\infty > K\sqrt{r/q} > Y_\infty > Kr/q$.
- If $\sigma = \sigma^*$, the boundaries intersect at $\tau^* = \infty$, and $B_\infty = Y_\infty = K\sqrt{r/q}$.

Proof. Follows from the perpetual American option formulas in Appendix A. ■

Proposition 1 is consistent with the results in [2], although we state it in different terms and use a simpler proof. A particular highlight is the observation that sufficiently high volatility ($\sigma > \sigma^*$) will result in the exercise interval being pinched off at some finite maturity value τ^* , wherefore it is never optimal to exercise an option with maturity $\tau > \tau^*$.

There appears to be no closed-form expression for τ^* , although we know⁷ that it will decrease in σ . In practice, it would be useful to at least establish whether the boundaries intersect in some pricing interval $[t, T]$; i.e., if $\tau^* < T - t$. Even this, we believe, cannot be answered definitively without first computing the option price (see “Computational method” section below), yet we can easily obtain an a priori upper bound on τ^* from the properties of European options (see also Proposition 2.5 in [2]):

Lemma 1. For the American double-boundary case we have, for both puts and calls:

$$\tau^* < \hat{\tau} \triangleq \hat{\sigma}^{-1}(\sigma), \quad (3)$$

with

$$\hat{\sigma}(\tau) \triangleq \frac{|\Phi^{-1}(e^{q\tau}) - \Phi^{-1}(e^{r\tau})|}{\sqrt{\tau}}. \quad (4)$$

Proof. Consider, say, a call option and form the function

$$f(\tau, S) = v(\tau, S) - (S - K) = S(e^{-q\tau}\Phi(d_+(\tau, S/K)) - 1) - K(e^{-r\tau}\Phi(d_-(\tau, S/K)) - 1).$$

Since v (the European call option) is a convex function of S , f has a global minimum at a finite $S^* > 0$ satisfying $f_S(\tau, S^*) = 0$. The European option also has positive vega and it is easy to see that there must be a unique $\hat{\sigma}(\tau)$ for which $f(\tau, S^*) = 0$ as well. Combining $f = f_S = 0$ with $d_+ - d_- = \sigma\sqrt{\tau}$, we recover (4), an expression that is easily seen to also hold for the double-boundary put option case.

By the definition of f , if σ exceeds $\hat{\sigma}(\tau)$, a τ -maturity European option value will not intersect the exercise region, which must also be the case for the American option which is strictly larger than the European value in its continuation region. Equation (3) then follows. ■

Remark 1. In Lemma 1, $\hat{\tau}$ is sure to exist since $\lim_{\tau \rightarrow \infty} \hat{\sigma}(\tau) = \infty$ and (from L'Hôpital's rule and a few manipulations) $\lim_{\tau \rightarrow \infty} \hat{\sigma}(\tau) = \sigma^*$.

The quantity $\hat{\tau}$ can be computed from (3) by standard numerical root-search. To avoid cancellation in (4), for computer-coding purposes it is best to use

$$\Phi^{-1}(\exp(\alpha\tau)) = -\Phi^{-1}(-\expm1(\alpha\tau)), \quad \alpha \in \{r, q\},$$

Table 1: American call option boundary asymptotes

q	r	B_0	Y_0	B_∞	Y_∞
$q > 0$	$r \in \mathbb{R}$	$K \max(1, r/q)$	∞	$K \frac{\lambda_+}{\lambda_+ - 1}$	∞
$q = 0$	$r \geq 0$	∞	∞	∞	∞
$q = 0$	$r < 0$	K	∞	$K \frac{\lambda}{\lambda - 1}, \sigma < \sigma^*$ $\infty, \sigma \geq \sigma^*$	∞
$q < 0$	$r \geq 0$	∞	∞	∞	∞
$q < 0$	$r < q < 0$	K	Kr/q	$K \frac{\lambda_+}{\lambda_+ - 1}, \sigma < \sigma^*$ $K\sqrt{r/q}, \sigma = \sigma^*$	$K \frac{\lambda_-}{\lambda_- - 1}, \sigma < \sigma^*$ $K\sqrt{r/q}, \sigma = \sigma^*$
$q < 0$	$q \leq r < 0$	∞	∞	∞	∞

where we recall that $\expm1(x)$ is defined as $\exp(x) - 1$ and is readily available in most programming languages.

While we do not carry out further analysis here, we note in passing that the result in Lemma 1 can possibly be sharpened if we use other instruments than European options (e.g., barrier or compound options) to establish the bound for τ^* . All we need to carry out the proof is that the price of any comparative instrument can never exceed that of the American option value.

Summary of results for all configurations of r and q

The analysis in the preceding two sections can be carried out for all possible configurations of r and q in \mathbb{R}^2 . Results for American call options are listed in Table 1, using the notation

$$\lambda_{\pm} = \frac{-\mu \pm \sqrt{\mu^2 + 2r\sigma^2}}{\sigma^2}, \quad \mu = r - q - \frac{\sigma^2}{2}, \quad \lambda = \frac{-2r}{\sigma^2}.$$

For additional insight into the properties of the exercise region, the results in the table should be supplemented with the fundamental monotonicity result

$$\frac{\partial B(\tau)}{\partial \tau} > 0, \quad \frac{\partial Y(\tau)}{\partial \tau} < 0, \quad (5)$$

whenever B and Y exist. Further, Appendix A lists the values of the perpetual American options for those cases where the values are well-defined.

Besides the double-boundary case $r < q < 0$, for American call options a notable non-standard case arises for the case where $r < q = 0$. This is a single-boundary case where the perpetual option boundary can reach ∞ (for $\sigma \geq \sigma^* = \sqrt{-2r}$); even so, the perpetual value is well-defined and finite. This begs the question whether, for sufficiently high volatilities, there might be a finite maturity τ^* for which the exercise boundary ceases to exist (as in: goes to infinity). This turns out *not* to be the case: the exercise boundary will be finite for all finite τ , and only the limit of the boundary for $\tau \rightarrow \infty$ will be infinite.⁸

Table 1 holds for the American call option, but can be converted to American puts using put–call symmetry. Results are listed in Table 2 for completeness, with the monotonicity result (5) for puts being $\partial B(\tau) / \partial \tau < 0$, $\partial Y(\tau) / \partial \tau > 0$.

OPTION PRICING

Table 2: American put option boundary asymptotes⁹

r	q	B_0	Y_0	B_∞	Y_∞
$r > 0$	$q \in \mathbb{R}$	$K \max(1, r/q)$	0	$K \frac{\lambda_-}{\lambda_- - 1}$	0
$r = 0$	$q \geq 0$	0	0	0	0
$r = 0$	$q < 0$	K	0	$K \frac{\lambda}{\lambda - 1}, \quad \sigma < \sigma^*$ $0, \quad \sigma \geq \sigma^*$	0
$r < 0$	$q \geq 0$	0	0	0	0
$r < 0$	$q < r < 0$	K	Kr/q	$K \frac{\lambda_-}{\lambda_- - 1}, \quad \sigma < \sigma^*$ $K\sqrt{r/q}, \quad \sigma = \sigma^*$	$K \frac{\lambda_+}{\lambda_+ - 1}, \quad \sigma < \sigma^*$ $K\sqrt{r/q}, \quad \sigma = \sigma^*$
$r < 0$	$r \leq q < 0$	0	0	0	0

Integral representation for the double-boundary case

In this section, we focus on the American put, since this will be the most useful for computational purposes. Ref. [1] contains a full discussion of the classical integral representations for American options with a single exercise boundary, as originally stated in, e.g., [12] and [4]. The following proposition extends the basic result to more complicated exercise regions:

Proposition 2. Consider an American put¹⁰ option in the Black–Scholes model described in the section above. Let the exercise region at time t be denoted $\mathcal{A}(t)$ i.e., exercise at time t is optimal if $S(t) \in \mathcal{A}(t)$. Then, for all values of r and q in \mathbb{R}^2

$$V(\tau, S) = v(\tau, S) + \int_0^\tau e^{-r(\tau-u)} \mathbb{E} \{ 1_{\{S(T-u) \in \mathcal{A}(T-u)\}} (rK - qS(T-u)) \mid S(t) = S \} du. \quad (6)$$

Proof (sketch): For a given maturity T and strike K , let $P(t, S)$ be the time- t value of the American put option, written as a function of t and S (such that $P(t, S) = V(T-t, S)$). Form the function $H(t) = e^{-rt} P(t, S)$ and note that $P(t, S(t)) = K - S(t)$ whenever $S(t) \in \mathcal{A}(t)$. Ito's lemma implies that (omitting arguments to P)

$$dH(t) = 1_{\{S(t) \in \mathcal{A}(t)\}} \{ -e^{-rt} dS(t) - re^{-rt} (K - S(t)) dt \} + 1_{\{S(t) \notin \mathcal{A}(t)\}} \sigma e^{-rt} S(t) \frac{\partial P}{\partial S} dW(t), \quad (7)$$

where we have relied on continuity of P across the exercise boundary, and on the lack of local time accumulation at the boundary due to smooth pasting conditions [see (14) below]. Integrating (7) from t to T , taking expectations, and using $H(t) = e^{-rt} (K - S(T))$ we get

$$P(t, S) = p(t, S) + rK \int_t^T e^{-r(s-t)} \mathbb{E}(1_{\{S(s) \in \mathcal{A}(s)\}} \mid S(t) = S) ds - q \int_t^T e^{-r(s-t)} \mathbb{E}(1_{\{S(s) \in \mathcal{A}(s)\}} S(s) \mid S(t) = S) ds, \quad (8)$$

where $p(t, S)$ is the European put option price. Setting $u = T - s$ (and recalling $\tau = T - t$) leads to (6). ■

Given (6), we can easily work through the various cases in Table 2, comput-

ing the required integrands of (6) in closed form. Here, we only need the double-boundary case $r < q < 0$ where, as shown earlier, $\mathcal{A}(s) = [Y(T-s), B(T-s)]$.

To simplify expressions in the sequel, let $p(\tau, S, K)$ and $c(\tau, S, K)$ be the European put and call prices for strike K . Then

$$p_S(\tau, S, K) = -e^{-q\tau} \Phi(-d_+(\tau, S/K)), \quad c_S(\tau, S, K) = e^{-q\tau} \Phi(d_+(\tau, S/K)), \quad (9)$$

$$p_K(\tau, S, K) = e^{-r\tau} \Phi(-d_-(\tau, S/K)), \quad c_K(\tau, S, K) = -e^{-r\tau} \Phi(d_-(\tau, S/K)). \quad (10)$$

Also

$$p_{SS} = c_{SS} = p_{KK} = c_{KK} = \frac{e^{-q\tau}}{S\sigma\sqrt{\tau}} \phi(d_+(\tau, S/K)) = \frac{Ke^{-r\tau}}{S^2\sigma\sqrt{\tau}} \phi(d_-(\tau, S/K)). \quad (11)$$

Corollary 1. When $q < r < 0$, the American put option satisfies

$$V(\tau, S, K) = p(\tau, S, K) + rK \int_0^{\min(\tau, \tau^*)} [p_K(\tau - u, S, B(u)) - p_K(\tau - u, S, Y(u))] du + qS \int_0^{\min(\tau, \tau^*)} [p_S(\tau - u, S, B(u)) - p_S(\tau - u, S, Y(u))] du, \quad (12)$$

where τ^* is a finite number for $\sigma > \sigma^*$, and $\tau^* = \infty$ if $\sigma \leq \sigma^*$.

We skip the obvious proof of Corollary 1, but note that it holds for all S (whether in the exercise region or not) and all τ (whether before or after τ^*). If we constrain the regions of S and τ , additional results are possible. For instance, when S is in the continuation region (but not when it is in the exercise region), the American put price $V(\tau, S)$ for $q < r < 0$ also satisfies the classical partial differential equation (PDE)

$$V_\tau = \frac{1}{2} \sigma^2 S^2 V_{SS} - rKV_K - qSV_S,$$

subject to the value-match conditions

$$V(\tau, B(\tau)) = K - B(\tau), \quad V(\tau, Y(\tau)) = K - Y(\tau). \quad (13)$$

and to the smooth pasting conditions

$$V_S(\tau, B(\tau)) = V_S(\tau, Y(\tau)) = -1. \quad (14)$$

If we consider only values of S in the continuation region and additionally require $\tau < \tau^*$ then we may simplify Corollary 1 in the following manner:

Corollary 2. When $q < r < 0$ and $\tau \leq \tau^*$, for $S \geq B(\tau)$ the American put value satisfies

$$V(\tau, S, K) = p(\tau, S, K) + \int_0^\tau [rKp_K(\tau - u, S, B(u)) + qSp_S(\tau - u, S, B(u))] du. \quad (15)$$

And for $S \leq Y(\tau)$ it satisfies

$$V(\tau, S, K) = K - S - \int_0^\tau [rKp_K(\tau - u, S, Y(u)) + qSp_S(\tau - u, S, Y(u))] du. \quad (16) \quad \square$$

OPTION PRICING

Proof: When $S > B(\tau)$ and $\tau \leq \tau^*$, we know that $B(u) > Y(u)$ for all $u < \tau$ and exercise can never happen when S hits Y (since B will always be hit first). We may therefore remove Y entirely from the proof of Proposition 2, simply using $\mathcal{A}(t) = \{S : S \leq B(T - t)\}$. With smooth pasting at B , this yields (15). For $S \leq B(\tau)$ these same arguments lead to

$$K - S = p(\tau, S, K) + \int_0^\tau [rKp_K(\tau - u, S, B(u)) + qSp_S(\tau - u, S, B(u))] du, \quad S \leq B(\tau). \quad (17)$$

Equation (17) holds for all $S \leq B(\tau)$, including those S for which $S \leq Y(\tau)$. Clearly, (12) also holds for $S \leq Y(\tau)$, and combining (17) and (12) leads to (16). ■

The result in Corollary 2 is very convenient, as (15) and (16) allow one to establish two decoupled equations for the exercise boundaries B and Y , allowing us to reuse some of the single-boundary iteration methods of [1] with minimal changes. We discuss this next.

Computational method

Our objective is to adapt the algorithm in [1] to cover all possible configurations of r and q in Tables 1 and 2. We focus on the American put, which is often more convenient to implement in numerical schemes; the American call can then be handled by symmetry (e.g., [7]):

$$V_{\text{call}}(\tau, S; K, T, r, q) = V_{\text{put}}(\tau, K; S, T, q, r), \quad (18)$$

$$B_{\text{call}}(\tau; K, r, q) = K S/B_{\text{put}}(\tau; S, q, r), \quad Y_{\text{call}}(\tau; K, r, q) = K S/Y_{\text{put}}(\tau; S, q, r). \quad (19)$$

In Table 2, the method in [1] can handle all cases for which the American put differs from the European put, except¹¹ for the double-boundary case $q < r < 0$. We thus focus exclusively on this case going forward.

Fixed-point iterations

Proceeding as in [1], our intent is to determine both B and Y from fixed-point iterations of the form

$$X(\tau) = K \frac{N_X(\tau; B, Y)}{D_X(\tau; B, Y)}, \quad \tau \leq \min(T - t, \tau^*), \quad X \in \{B, Y\}. \quad (20)$$

As explained in [1], we have many ways of creating such iterations. For instance, if we combine the value-match condition (13) with Corollary 3 and rearrange, we get

$$N_X(\tau; B, Y) = -c_K(\tau; X(\tau), K) + r \int_0^\tau [-c_K(\tau - u, X(\tau), B(u)) + p_K(\tau - u, X(\tau), Y(u))] du, \quad (21)$$

$$D_X(\tau; B, Y) = c_S(\tau; X(\tau), K) + q \int_0^\tau [c_S(\tau - u, X(\tau), B(u)) - p_S(\tau - u, X(\tau), Y(u))] du, \quad (22)$$

Notice that N_X and D_X in (21) and (22) depend on both B and Y , wherefore a fixed-point iteration on (20) would require one to solve for both boundaries simultaneously in a single joint iteration scheme. While this is certainly doable,¹² it is easier, and significantly more accurate, to use Corollary 2 to split the problem into two separate fixed-point iterations. For instance, if we set $S = B(\tau)$ in (15), we get another value-match iteration for B , for $\tau \leq \tau^*$:

$$N_B(\tau, B) = -c_K(\tau, B(\tau), K) - r \int_0^\tau c_K(\tau - u, B(\tau), B(u)) du, \quad (23)$$

$$D_B(\tau, B) = c_S(\tau, B(\tau), K) + q \int_0^\tau c_S(\tau - u, B(\tau), B(u)) du, \quad (24)$$

which no longer involves Y . We will designate the usage of (23) and (24) in (20) as *fixed-point system B* (or *FP-B* for short).

We can use the value-match principle on (15) to find a similar fixed-point system for Y , but bulk numerical experiments show that it is typically better to use smooth pasting to find Y . For this, we differentiate (16) with respect to S ; substitute $S = Y(\tau)$; apply (14); and rearrange, for $\tau \leq \tau^*$:

$$N_Y(\tau, Y) = rK \int_0^\tau c_{KK}(\tau - u, Y(\tau), Y(u)) du, \quad (25)$$

$$D_Y(\tau, Y) = qY \int_0^\tau c_{SS}(\tau - u, Y(\tau), Y(u)) du + q \int_0^\tau p_S(\tau - u, Y(\tau), Y(u)) du, \quad (26)$$

where $\phi(x) = \frac{1}{\sqrt{2\pi}} e^{-x^2/2}$ is the Gaussian PDF.

Equations (25) and (26) do not depend on B and, together with (20), form a fixed iteration for the Y boundary; we denote this *fixed-point system Y* (or *FP-Y* for short).

We notice that both (23) and (24), and (25) and (26), only hold for $\tau \leq \tau^*$, where τ^* is the point where the B and Y intersect (assuming they do so). In practice, we just run the two separate iterations for B and Y for all relevant τ , and then discover τ^* as the point where B and Y intersect, provided that this happens inside $T - t$. Both $B(\tau)$ and $Y(\tau)$ can then be set to 0 for all $\tau > \tau^*$.

The right-hand side of (20) can occasionally be negative; in practice, we have only observed this with FP-B. When this happens, one can just skip the update to $B(\tau)$ with no ill effect, but it is possible to do a little better by rearranging (20) as

$$B = B + KN_B - BD_B \quad (27)$$

and then use this as an alternate way to update $B(\tau)$ so that the step is not wasted.

Once the boundaries B and Y are computed up to $\min(T - t, \tau^*)$, the option value $V(T - t, S(\tau))$ may be obtained from (12) by numerical integration.

Domain transformations and quadrature

The accuracy and stability of the method is improved by transforming the time domain to square-root space:

$$z = \sqrt{u}, \quad du = 2z dz.$$

It is straightforward to adjust the integrals in (23) and (24), and (25) and (26), accordingly, following the general rule

OPTION PRICING

$$\int_0^{\tau} f(u) du = 2 \int_0^{\sqrt{\tau}} f(z^2) z dz.$$

In an implementation, it is also convenient to work with log-spot rather than spot, and to normalize log-strike to zero. Then the computation is done in terms of the transformed boundaries

$$\widehat{B}(z) = \ln(B(z^2) / B_0), \quad \widehat{Y}(z) = \ln(Y(z^2) / Y_0).$$

Full algorithm for double-boundary American put

As in [1], the computational complexity of the algorithm will be defined by three constants: the number of quadrature points (l); the number of fixed-point iterations (m); and the number of collocation points (n). The algorithm proceeds as follows:

1. Define the maturity range as $\bar{\tau} = \min(T - t, \hat{\tau})$, where $\hat{\tau}$ is given in (3).
2. Generate n Chebyshev nodes for $[0, \sqrt{\bar{\tau}}]$, and initialize two n -point Chebyshev interpolators \widehat{B} and \widehat{Y} with flat values K and Kr/q .
3. Execute m iterations for \widehat{B} and \widehat{Y} , using the FP-B and FP-Y schemes, respectively.¹³ The iterations are executed at all Chebyshev nodes (i.e., at the *collocation points*); and integrals in (23) and (24), and (25) and (26), are computed by l -point numerical quadrature.
4. After Step 3, we may treat (by Chebyshev interpolation) \widehat{B} and \widehat{Y} as continuous functions that can be evaluated on $[0, \sqrt{\bar{\tau}}]$. We can test whether¹⁴ these functions intersect inside $[0, \sqrt{\bar{\tau}}]$ and, if so, use a standard zero-finder (the Brent algorithm, say) to solve $\widehat{B}(z^*) = \widehat{Y}(z^*)$.
5. If an intersection is computed in Step 4, set $\tau^* = (z^*)^2$. Otherwise, set $\tau^* = T - t$.
6. Compute the option value $V(T - t, S(t))$ from:
 - eq (12), if $T - t > \tau^*$,
 - eq (15), if $T - t = \tau^*$ and $S(t) > B(T - t)$,
 - eq (16), if $T - t = \tau^*$ and $S(t) < Y(T - t)$.

Otherwise,¹⁵ set $V(T - t, S(t)) = K - S(t)$.

Some practical tips and extensions

- If $\sigma < \sigma^*$, we can use the B_∞ and Y_∞ results of Table 2 to both improve the initial guess and ensure that the fixed-point iterations for boundaries B and Y do not extend below the long-maturity asymptotes.
- In contrast to the single-boundary case, where both perform well, here tanh-sinh quadrature (see [1] for details) is significantly better than Gauss-Legendre.
- Although the algorithm above used the same values of l , m , n for both boundaries B and Y , this is not necessary. As the Y boundary is flatter than the B boundary (this is shown in Figure 2 below), in fact it is more efficient to use fewer iterations and collocation points (say, half as many) for Y as for B .
- In the fixed-point iterations, the number of quadrature points can, for instance, be set to $l = 2n + 1$, which gives good results in most cases.
- For the final integral to compute the option price, it is important to use a fairly large number of quadrature points, for instance 257. This has negligible impact on speed, so there are no reasons to skimp here.
- For the B boundary, using $m = 16$ fixed-point iterations works well; for the Y boundary, we can easily get away with half this number.

- For each fixed-point iteration, the monotonicity of the boundaries should be enforced at the Chebyshev nodes. At the end of the j -th iteration one can set $B_i^{(j)} = \min(B_i^{(j)}, B_{i-1}^{(j)})$, and $Y_i^{(j)} = \max(Y_i^{(j)}, Y_{i-1}^{(j)})$, for $i = 1, \dots, n - 1$.

Numerical results Some visualizations

To visualize the double-boundary exercise region, Figure 1 shows the value function for a long-dated American put option where the exercise region is a finite interval. Notice in particular the existence of a boundary Y below which it is no longer optimal to exercise the American put.

In Figure 2, we show a case where the double-boundary exercise region for an American put gets pinched off at a finite time τ^* . As discussed earlier, the exercise region decreases monotonically in size up to τ^* .

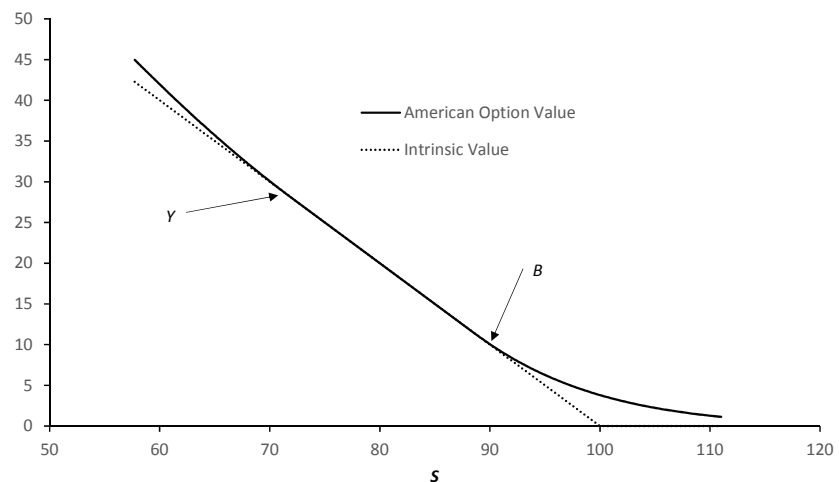
Some convergence results

Before turning to a bulk test in the next subsection, let us quickly show some representative convergence results for the price of an American put. We use the process settings of Figure 2 with $S(t) = 100$. The option strike is $K = 100$, and we let the maturity vary from 45 days to 3600 days. We also vary the number of collocation points from $n = 4$ to $n = 16$. In all tests, for a given n we follow the advice in the above subsection “Some practical tips and extensions” and set the number of integration nodes l equal to $2n + 1$, the number of fixed-point iterations¹⁶ m to 16, and use 257 quadrature nodes for the final integral for the option value.

As Table 3 shows, convergence is very rapid, with doubling of numerical efforts often leading to precision improvements of several orders of magnitude. Also, relative errors are small – and easily within tolerances sufficient for practical pricing purposes – even at very modest values for the number of collocation points (and equally modest number of iterations and number of quadrature points).

To quickly get a feel for how the results of Table 3 compare to alternative methods, we ran a (very expensive) 5000×5000 second-order PDE solver to compute the val-

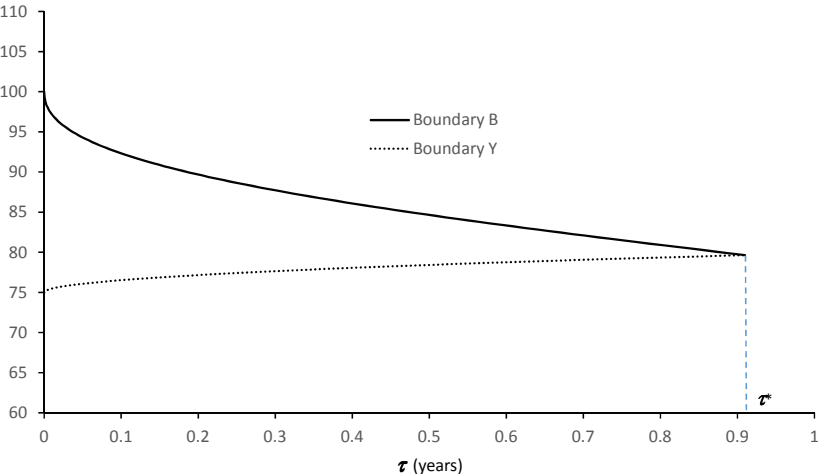
Figure 1: American put option value as a function of stock price S



Process parameters: $r = -5\%$, $q = -7.5\%$, $\sigma = 7.5\%$. Option contract: $T - t = 5$ years, $K = 100$.

OPTION PRICING

Figure 2: Exercise boundaries $B(\tau)$ and $Y(\tau)$ for American put option



Process parameters: $r = -1.2\%$, $q = -1.6\%$, $\sigma^* = 10.0\%$. Option contract: $K = 100$. The critical volatility is $\sigma^* \approx 0.02396610$.

Table 3: Convergence of double-boundary American put option price

n	$T - t$ (days)	Value V	Rel. error
4	45	1.380529947	2.28E-06
6	45	1.380533148	4.24E-08
8	45	1.380533090	1.64E-10
16	45	1.380533089	3.87E-10
4	90	1.942375452	2.98E-06
6	90	1.942381299	3.17E-08
8	90	1.942381244	3.43E-09
16	90	1.942381237	4.88E-10
4	180	2.729256541	3.92E-06
6	180	2.729267306	1.99E-08
8	180	2.729267270	6.53E-09
16	180	2.729267252	1.49E-10
4	360	3.830499059	5.57E-06
6	360	3.830520503	2.77E-08
8	360	3.830520455	1.51E-08
16	360	3.830520425	7.22E-09
4	3600	12.189454779	1.01E-05
6	3600	12.189316380	1.27E-06
8	3600	12.189317409	1.18E-06
16	3600	12.189323541	6.79E-07

Convergence of the algorithm in the subsection “Full algorithm for double-boundary American put” for an American put option with strike $K = 100$. The number of collocation points n ranges from 4 to 16, with $m = 16$ and $l = 2n + 1$. The option maturities τ range from 45 days to 3600 days, with each day being $1/365$ of a year. Along with the option values, we also list the absolute value of the relative error (“Rel. error”), using benchmark prices computed by a high-precision setting of $(m, n, l) = (64, 128, 257)$. Process parameters as in Figure 2: $r = -1.2\%$, $q = -1.6\%$, $\sigma = 10.0\%$.

ues of the American put at $S = 101$. The relative error across the various maturities in the table was around $7.0\text{E-}7$, comparable in precision to our scheme when run with n somewhere around 4 or 5. Consistent with the results in [1], we thus find that the fixed-point iteration scheme is orders of magnitude faster than grid- or PDE-based methods.

A bulk test

While we do not intend to be as thorough in our testing as in [1], we still want to finish this section with a bulk test where we record summary precision statistics for our algorithm across a range of process parameters and option contract terms. We lock the strike at $K = 100$ and vary all other parameters through the parameter ranges listed in Table 4. When creating parameter combinations for test purposes, we ignore the following cases: 1) $q > r$; 2) the option value equals intrinsic value; or 3) the option value is less than $1.0\text{E-}8$. As it turns out, this results in a total of 3242 valid test cases (1990 short-dated and 1254 long-dated). Summary statistics for pricing errors across the test cases are listed in Table 5, as a function of the dimensioning of the numerical method.

Table 5 confirms on a much broader set of options the conclusions arrived at from Table 3: highly accurate price results can be obtained with only a modest number of collocation and integration nodes. Moreover, the bulk test shows that our proposed scheme is robust, as the maximum errors (and maximum relative errors) are both small and relatively close to the average errors.

Conclusion

In this article, we provided the necessary theory, asymptotics, and algorithms to allow the fixed-point iteration method in [1] to be extended to negative rates and dividends, even when the exercise region splits into two separate boundaries. For this “double-boundary” case, in particular, we were able to design iteration schemes that conveniently split into separate, uncoupled iterations for each boundary. We demonstrated with numerical examples that the scheme has spectral convergence and can compute prices of American options with a double boundary with great precision and efficiency.

While our focus here was on the constant-parameter Black–Scholes model, one can show that many results carry over to time-dependent rates, dividends, and volatilities. If the time dependence is strong or irregular, the exercise region can in principle be very complicated, but convexity ensures that it will *locally* always be a closed interval. In the interests of conciseness, we leave the treatment of time dependence as a topic for future research. Extension of the dynamics to non-lognormal processes is another interesting topic for the future.

Table 4: Parameter ranges for bulk test

Parameter	Values
r	$\{-0.0009, -0.0049, -0.0099, -0.0199, -0.0499\}$
q	$\{-0.001, -0.005, -0.01, -0.02, -0.05\}$
S	$\{50, 85, 95, 100, 105, 115, 150, 200\}$
σ	$\{0.05, 0.1, 0.2, 0.5\}$
T (years), short-dated	$\{7/365, 30/365, 91/365, 182/365, 273/365, 1\}$
T (years), long-dated	$\{2, 3, 5\}$

Table 5: Results of bulk test

Short-dated:	<i>n</i> =4	<i>n</i> =6	<i>n</i> =8	<i>n</i> =10	<i>n</i> =12	<i>n</i> =16	<i>n</i> =32
RMSE	8.1E-05	1.2E-05	4.5E-06	1.5E-06	6.9E-07	3.5E-07	3.6E-07
RRMSE	8.8E-05	9.2E-05	2.1E-06	4.8E-07	1.3E-07	3.8E-08	1.6E-08
MAE	1.0E-03	1.6E-04	6.2E-05	2.1E-05	1.4E-05	1.1E-05	1.1E-05
MRE	1.6E-03	9.2E-05	4.5E-05	1.2E-05	1.7E-06	7.5E-07	2.2E-07
Long-dated:	<i>n</i> =4	<i>n</i> =6	<i>n</i> =8	<i>n</i> =10	<i>n</i> =12	<i>n</i> =16	<i>n</i> =32
RMSE	6.9E-04	9.8E-05	2.4E-05	8.2E-06	4.3E-06	2.7E-06	2.6E-06
RRMSE	7.6E-04	9.2E-05	1.7E-05	3.3E-06	2.0E-06	5.1E-07	8.1E-08
MAE	1.3E-02	1.8E-03	3.0E-04	7.6E-05	5.2E-05	5.1E-05	5.0E-05
MRE	1.4E-02	1.9E-03	3.3E-04	3.5E-05	3.1E-05	1.2E-05	8.7E-07

Convergence of the algorithm in the subsection “Full algorithm for double-boundary American put” for an American put option with strike $K = 100$. The number of collocation points n ranges from 4 to 32, with $n = 16$ and $l = 2n + 1$. Model and contract parameter ranges are as given in Table 4, with computation error results filtered as described in the text. Results are reported separately for short-dated options (maturities less than 1 year) and long-dated options. Benchmark prices were computed by a high-precision setting of $(m, n, l) = (64, 128, 257)$. Error statistics reported are: RMSE (root mean square error); RRMSE (root mean square of relative errors); MAE (maximum absolute error); and MRE (maximum relative error).

Appendix A: Perpetual American options with negative rates and dividends

For positive rates and dividends, perpetual American option prices for the Black–Scholes model were first given in [13]. In this appendix, we extend the results to also cover non-positive values of r and q , focusing on the “new” cases in Table 1. For brevity, we list all results without proof, but note that all results follow from ordinary differential equation techniques similar to those in [13].

Double-boundary case ($r < q < 0$)

Given $r < q < 0$, define

$$\sigma^* = \sqrt{-2r} - \sqrt{-2q}, \quad \mu = r - q - \frac{\sigma^2}{2}, \quad \lambda_{\pm} = \frac{-\mu \pm \sqrt{\mu^2 + 2r\sigma^2}}{\sigma^2}. \tag{A.1}$$

For $0 < \sigma < \sigma^*$:

$1/(1 - q/r) < \lambda_- < 1/(1 - \sqrt{q/r}) < \lambda_+ < \infty$,
and the perpetual American call price is

$$V(S) = \begin{cases} (B_{\infty} - K)(S/B_{\infty})^{\lambda_+}, & S \leq B_{\infty} = \frac{\lambda_+}{\lambda_+ - 1}K, \\ S - K, & B_{\infty} < S < Y_{\infty}, \end{cases}$$

We demonstrated with numerical examples that the scheme has spectral convergence and can compute prices of American options with a double boundary with great precision and efficiency

$$(Y_{\infty} - K)(S/Y_{\infty})^{\lambda_-}, \quad S \geq Y_{\infty} = \frac{\lambda_-}{\lambda_- - 1}K. \tag{A.2}$$

When $\sigma = \sigma^*$, $\lambda_- = \lambda_+$, $= 1/(1 - \sqrt{q/r})$, and (A.2) simplifies to

$$V(S) = (H - K)(S/H)^{\frac{H}{H-K}}, \quad 0 < S < \infty, \quad B_{\infty} = Y_{\infty} = H = K\sqrt{r/q}. \tag{A.3}$$

For $\sigma > \sigma^*$, λ_{\pm} are imaginary; the value of the perpetual is infinite. The put formulas are obtained from American put–call symmetry.

A special single-boundary case ($r < q = 0$)

Given $r < q = 0$, let $\lambda = -2r/\sigma^2$. The perpetual American call price is

$$V(S) = \begin{cases} S, & \lambda \leq 1, \\ (B_{\infty} - K)(S/B_{\infty})^{\lambda}, & \lambda > 1, \quad S \leq B_{\infty} = \frac{\lambda}{\lambda - 1}K, \\ S - K, & \lambda > 1, \quad S > B_{\infty}. \end{cases} \tag{A.4}$$

The put formulas are, once again, obtained from American put–call symmetry.

The standard single-boundary case ($q > 0$)

For completeness, the perpetual American call price in the standard case is

$$V(S) = \begin{cases} S - K, & S > B_{\infty}, \\ (B_{\infty} - K)(S/B_{\infty})^{\lambda_+}, & S \leq B_{\infty}, \end{cases} \quad B_{\infty} = \frac{\lambda_+}{\lambda_+ - 1}K, \quad 1 < \lambda_+ < \infty. \tag{A.5}$$

The put formulas are analogous:

$$V(S) = \begin{cases} K - S, & S < B_{\infty}, \\ (K - B_{\infty})(S/B_{\infty})^{\lambda_-}, & S \geq B_{\infty}, \end{cases} \quad B_{\infty} = \frac{\lambda_-}{\lambda_- - 1}K, \quad -\infty < \lambda_- < 0. \tag{A.6}$$



OPTION PRICING

ENDNOTES

1. The timing results in our article were computed using a straightforward implementation in C++. We have subsequently improved the performance roughly tenfold, mostly by organizing the code to exploit instruction-level parallelism and by vectorizing calls to elementary math functions.
2. Technically, the polynomial is best expressed in powers of square-root of maturity (see the “Domain transformations and quadrature” subsection).
3. Details of this scheme are for another day, but the reader can get some inspiration from [9].
4. This is generally true in diffusion models with deterministic rates and applies to any European, Bermudan, or American option with a convex payout. Some additional technical conditions are required to ensure that the discounted asset price is a martingale. See [8], [11], and [10].
5. See [5] for a more precise statement. As shown in [6] (see also [1]), it is not the case that the boundary always has uniform sign of its convexity (second derivative) as a function of τ .
6. A summary of results for all sign combinations of r and q can be found in Tables 1 and 2.
7. This follows because American options have positive vega in the continuation region (see [3]).
8. If the boundary blows up at τ^* , it cannot exist for $\tau \geq \tau^*$ as this would lead to a violation of $V_\tau \geq 0$. In contrast, there cannot be a non-empty open time interval with no exercise as this would result in an American option price below intrinsic value.
9. For a put we have $\lambda_\pm = \frac{-\mu \pm \sqrt{\mu^2 + 2q\sigma^2}}{\sigma^2}$, $\mu = q - r - \frac{\sigma^2}{2}$, $\lambda = \frac{-2q}{\sigma^2}$, $\sigma^* = \sqrt{-2q} - \sqrt{-2r}$.
10. We focus on the American put, since this tends to be the most useful for computational purposes. The integral representation for a call can easily be established in the same manner.
11. In particular, the “new” single-boundary case $q < r = 0$ can be done by the technique in [1], with one slight caveat: the initial boundary guess used in [1] uses an analytical approximation that will fail if $r = 0$ is plugged in directly. One can either form a limit, use a small positive value for r , or simply start the iteration flat, by assuming $B(\tau) = K$ for all τ (and then possibly tack on a small number of extra iterations to compensate for the lack of a head start).
12. This is, for instance, the basis for the work in [15], a paper that was published while ours was under review. The algorithm in [15] is meant to be applied only when boundaries do not intersect. Our decoupled scheme based on Corollary 2 is not only faster than the joint scheme, it also has no problems dealing with intersecting boundaries. Our experience is also that using the decoupled FP-B and FP-Y systems with the stabilization (27) and then solving for τ^* as the intersection point of the two curves improves accuracy by three orders of magnitude over a joint iteration.
13. The iterations for \hat{B} and \hat{Y} can be done sequentially or in parallel, whatever is most convenient.
14. This will always be the case if $\hat{t} = \hat{\tau}$, but may also be the case if $\hat{\tau} = T - t$.
15. That is, $S(\tau)$ must be between B and Y , and hence in the exercise region.
16. We verified that the results did not change if we cut this number in half for the Y boundary, as described in the “Some practical tips and extensions” section.

REFERENCES

- [1] Andersen, L. B., Lake, M., and Offengenden, D. 2016. High-performance American option pricing. *Journal of Computational Finance* 20(1), 39–87.
- [2] Battauz, A., De Donno, M., and Sbuelz, A. 2015. Real options and American derivatives: the double continuation region. *Management Science* 61(5), 1094–1107.
- [3] Bergman, Y. Z., Grundy, B. D., and Wiener, Z. 1996. General properties of option prices. *The Journal of Finance* 51(5), 1573–1610.
- [4] Carr, P., Jarrow, R., and Myneni, R. 1992. Alternative characterizations of American put options. *Mathematical Finance* 2(2), 87–106.
- [5] Carr, P., and Lee, R. 2009. Put–call symmetry: extensions and applications. *Mathematical Finance* 19(4), 523–560.
- [6] Chen, X., Cheng, H., and Chadam, J. 2013. Non-convexity of the optimal exercise boundary for an American put option on a dividend-paying asset. *Mathematical Finance* 23, 169–185.
- [7] Detemple, J. 2001. American options: Symmetry properties. In E. Jouini, J. Cvitanic, and M. Musiela (eds), *Handbooks in Mathematical Finance: Topics in Option Pricing, Interest Rates and Risk Management*. Cambridge: Cambridge University Press, pp. 67–104.
- [8] Ekström, E. 2004. Properties of American option prices. *Stochastic Processes and their Applications* 114(2), 265–278.
- [9] Göttsche, O. and Vellekoop, M. 2011. The early exercise premium for the American put under discrete dividends. *Mathematical Finance* 21(2), 335–354.
- [10] Hobson, D. G. 1998. Volatility misspecification, option pricing and superreplication via coupling. *Annals of Applied Probability* 8, 193–205.
- [11] Janson, S. and Tysk, J. 2003. Volatility time and properties of option prices. *The Annals of Applied Probability* 13(3), 890–913.
- [12] Kim, I. J. 1990. The analytic valuation of American puts. *Review of Financial Studies* 3(4), 547–572.
- [13] Merton, R. 1973. The theory of rational option pricing. *Bell Journal of Economics and Management Science* 3(4), 141–183.
- [14] Staunton, M. 2020. Thanksgiving meal for Americans. *Wilmott* 108(July), 17–19.
- [15] Healy, J. 2021. Pricing American options under negative rates. *Journal of Computational Finance* 25(1), 1–27.

Book Club

Exclusive discounts on the latest books from Wiley... 30% off for *Wilmott magazine* readers!

Quantitative Financial Risk Management

Michael B. Miller

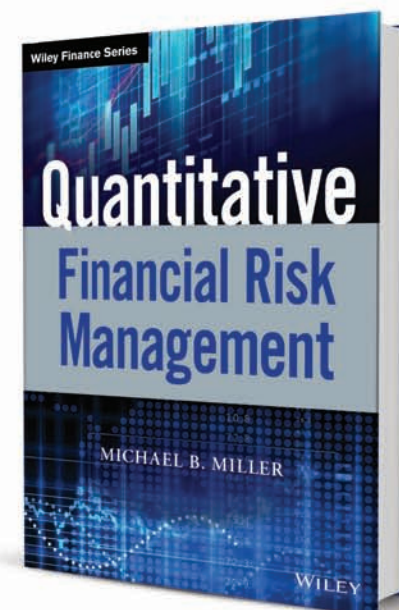
Our modern economy depends on financial markets, yet financial markets continue to grow in size and complexity. As a result, the management of financial risk has never been more important.

Quantitative Financial Risk Management is a textbook designed to teach students about financial risk management with an emphasis on financial models and mathematical techniques. Each chapter provides numerous sample problems and end-of-chapter questions. The book provides clear examples of how these models are used in practice and encourages students to think about the limits and appropriate use of financial risk models.

Topics covered include:

- Value at risk
- Stress testing
- Credit risk
- Liquidity risk
- Factor analysis
- Expected shortfall
- Copulas
- Extreme value theory
- Risk model backtesting
- Risk attribution
- Bayesian analysis
- and much more...

- 978-1-119-52220-1
- Hardback
- November 2018
- £65.00 / €72.70 / \$85.00
- **£45.50 / €50.89 / \$59.50**



Asymmetric Dependence in Finance Diversification, Correlation and Portfolio Management in Market Downturns

Jamie Alcock, Stephen Satchell

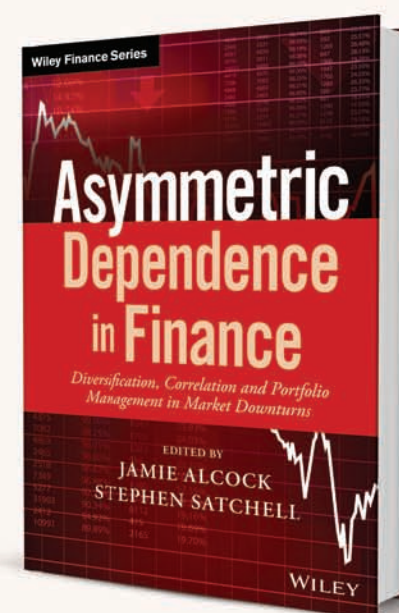
The Guide to Avoiding Downturn Vulnerability by Managing Correlation Dependency

Solidly grounded in quantitative finance research, *Asymmetric Dependence in Finance* is the definitive resource that offers an important analysis of the risks and benefits of asset correlation. The book spans the topics — managing asymmetric dependence using Copulas, to mitigating asymmetric dependence risk in real estate, credit and CTA markets — that comprise a survey of the most current tools available for measuring and managing this crucial issue.

With contributions from noted experts in the field, this book explores the risks and benefits of asset correlation and offers the most current strategies and models that can be implemented to protect investments that are no longer insulated from downturns by simply diversifying funds. It clearly shows that the relation between assets is much richer than previously thought, and correlation between returns is dependent on the state of the market. Correlations between assets significantly increase during market downturns compared to market upturns. The benefits of diversification collapse at the very time fund managers need to rely on diversification.

To help investors avoid financial disasters such as the 2008 global financial crisis and the 2006 hedge-fund crisis, the authors outline practical measures that can be implemented to boost fund performance and a proven strategy for putting in place an options-based approach that limits a portfolio's risk.

Written for fund managers, investors and financial officers, *Asymmetric Dependence in Finance* presents the most effective tools and strategies for improving fund, portfolio, and organization performance.



- 978-1-119-28901-2
- Hardback
- June 2018
- £80.00 / €90.40 / \$130.00
- **£56.00 / €63.28 / \$91.00**

SAVE 30%

When you subscribe to *WILMOTT magazine* you will automatically become a member of the **Wilmott Book Club** and you'll be eligible to receive 30% discount on specially selected books in each issue when you order direct from www.wiley.com - just quote promotion code **WILMO** when you order. The titles will range from finance to narrative non-fiction.

For further information, contact our **Customer Services Department** on +44 (0) 1865 778315, or Email: cs-journals@wiley.com